

STATISTICAL GEOMETRY AND CAVITY CORRELATIONS IN THE HARD SPHERE FLUID

Robin J. SPEEDY^{a,*} and Richard K. BOWLES^b

^a Apartment 504, 120 Courtenay Place, Wellington 6011, New Zealand;

e-mail: robin.speedy@clear.net.nz

^b Department of Chemistry, University of Saskatchewan, Saskatoon, S7N 5C9 Canada;

e-mail: richard.bowles@usask.ca

Received December 13, 2007

Accepted March 10, 2008

Published online April 2, 2008

Dedicated to Professor William R. Smith on the occasion of his 65th birthday.

The statistical geometry of a system of hard spheres is discussed in terms of the volumes V_j that lie with a sphere diameter, σ , of exactly j sphere centres. A site that has no sphere centre within σ is called a cavity site. We focus on the probability $n_{00}(r)$ that two sites separated by r are both cavity sites. $n_{00}(0)$, $n_{00}(\sigma)$, and the limiting slope $(d \ln n_{00}(r)/dr)_{r=0}$, are all known in terms of the thermodynamic properties. The V_j and $n_{00}(r)$ are measured by computer simulation and an empirical expression, which satisfies the known exact relations, is shown to represent $n_{00}(r)$ precisely in the range $0 \leq r \leq \sigma$.

Keywords: Statistical geometry; Cavity correlations; Hard spheres; Thermodynamics; Fluids; Computer simulation.

Boltzmann¹ foresaw that the dynamic and thermodynamic properties of simple fluids are largely determined by the repulsive forces between the molecules and that attractions play a lesser role. He discussed a gas of hard spheres, in which repulsions are represented by the geometrical condition that spheres cannot overlap, thus reducing the task of understanding the properties of simple fluids to its essence: statistical geometry. van der Waals' theory of the continuity of the liquid and gaseous states, and more recent perturbation theories of fluids^{2,3}, emphasise the essential correctness of Boltzmann's view, but, despite a century of effort, the central problem of understanding the statistical geometry of hard spheres has still to be solved.

In this section we define some geometrical quantities, explain relations between them, and show how they are related to the thermodynamic prop-

erties. The following sections report computer simulation calculations of some geometrical properties.

GEOMETRY

We consider a system of N hard spheres, each of diameter σ , with centres confined to a D dimensional space of volume V . The space is taken to be cubic in shape with periodic boundaries, so that the average structure about any point is independent of position. Each sphere excludes other sphere centres from the region within σ if its centre, as shown for discs ($D = 2$) in Fig. 1. The statistical geometry is discussed in terms of the volumes V_j that lie within σ of j , and only j , sphere centres⁴.

The space is subdivided, conceptually, into a lattice of V/ω very small cells, or sites⁴⁻⁷ each of volume ω , and a configuration is specified by a list of the N sites that locate a sphere centre. ω need not be specified more precisely, because it cancels out of all measurable properties and the limit $\omega \rightarrow 0$ can be taken implicitly. The number of configurations is denoted by $\Omega = \Omega(N, V, \sigma, \omega)$. The variable list (N, V, σ, ω) is omitted where no ambiguity arises.

$V_{j,k}$ is the volume within σ of j , and only j , sphere centres in configuration k , and $V_j = \langle V_{j,k} \rangle$ where $\langle \rangle$ denotes an average over the $k = 1, 2, \dots, \Omega$ configurations^{6,7}. $S_{j,k}$ is the surface area of $V_{j,k}$ and $S_j = \langle S_{j,k} \rangle$. A site within $V_{j,k}$ is called a V_j site. $n_j \equiv V_j/V$ is the probability that a random point is in a V_j site. A site that locates a sphere centre is called a c site. V_0 sites are called

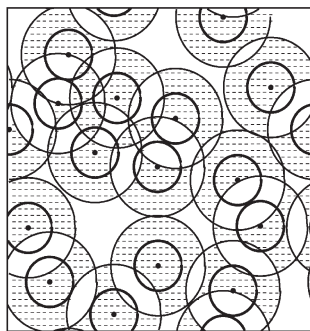


FIG. 1
16 discs in a square box with periodic boundaries. Small circles of diameter σ show the discs. Large circles of diameter 2σ show the exclusion discs. Regions overlapped by $j = 1$ or 3 exclusion discs are shaded

cavity sites, because a sphere can be added with its centre in $V_{0,k}$ without overlapping the other spheres. Boltzmann¹ called $V_{0,k}$ the "available space".

$\rho \equiv N/V$ is the number of spheres per unit volume, B_2 is the second virial coefficient, m is the maximum number of sphere centres that can fit within σ of a point ($m = 2$, $B_2 = \sigma$, $D = 1$; $m \leq 6$, $B_2 = \pi\sigma^2/2$, $D = 2$; $m \leq 12$, $B_2 = 2\pi\sigma^3/3$, $D = 3$).

For any configuration, and for the configurational averages,

$$\sum_{j=0}^m \frac{V_{j,k}}{V} = \sum_{j=0}^m n_j = 1. \quad (1)$$

The volume within σ of a site is $2B_2$, so the average number of sphere centres within σ of any site is

$$\sum_{j=0}^m \frac{jV_{j,k}}{V} = \sum_{j=0}^m jn_j = 2B_2\rho. \quad (2)$$

The surface area of all the exclusion spheres is

$$\sum_{j=0}^m S_{j,k} = \sum_{j=0}^m S_j = 2NDB_2/\sigma. \quad (3)$$

$n_{ij}(r)$ is defined as the probability that two sites separated by distance r are V_i and V_j sites. Site-site correlation functions $g_{ij}(r) = g_{ji}(r)$ are defined by

$$g_{ij}(r) \equiv \frac{n_{ij}(r)}{n_i n_j}, \quad i, j = 0, 1, \dots, m, c. \quad (4)$$

Kirkwood⁸ noted that a cavity site and a sphere centre are equivalent in the sense that their effect on the rest of the system is to exclude other sphere centres from a region of radius σ . The distribution of spheres about a cavity site (in a system of N spheres) is therefore the same as the distribution about a sphere centre (in a system of $N + 1$ spheres). The conditional probability that a site at distance r from a V_0 site is a V_j site is therefore⁴ (when $N \gg 1$)

$$n_j g_{0j}(r) = \begin{cases} n_j g_{0j}(r) & j = 0, 1, \dots, m, c, \quad r > \sigma \\ n_{j+1} g_{c(j+1)}(r) & j = 0, 1, \dots, m, \quad r < \sigma \end{cases}. \quad (5)$$

The probability that a site on the outside surface of an exclusion sphere is a V_j site is the limit of $n_j g_{0j}(r)$ as $r \rightarrow \sigma$ from $r > \sigma$, which is, from Eq. (5), $n_j g_{0j}(\sigma)$. The total area of all the exclusion surfaces is $2NDB_2/\sigma$ so the surface area of V_j is

$$S_j = (2NDB_2/\sigma) n_j g_{0j}(\sigma). \quad (6)$$

Figure 2 shows the volume excluded to sphere centres by a pair of cavity sites separated by distance r . The volume excluded is $2B_2$ when $r = 0$ and $4B_2$ when $r > 2\sigma$. The change in the volume excluded when the cavity sites are moved apart from $r = 0$ to $r \leq 2\sigma$, is

$$\Delta V(r) = \begin{cases} r, & D = 1 \\ 2\sigma^2 \{x(1-x^2)^{1/2} + \sin^{-1}(x)\}, & D = 2 \\ 2\pi\sigma^3 \{x - x^3/3\}, & D = 3 \end{cases} \quad (7)$$

where $x = r/2\sigma$.

Meeron and Siegert⁹ provide an elegant statistical mechanical analysis of the distribution functions for multiple cavities in fluids with continuous potentials, and they specialise their results to the case, considered here, of two cavities in a hard sphere fluid. The generality and rigour of their analysis is not required to understand the relations used in this paper, so we give simpler explanations of some of their results (Eqs (8)–(11) below) to show that they follow directly from geometrical considerations, without any recourse to statistical mechanics.

The conditional probability, $n_0 g_{00}(r)$, that a site at distance r from a cavity site is also a cavity site, must tend to unity as $r \rightarrow 0$, so⁴

$$n_0 g_{00}(0) = 1. \quad (8)$$

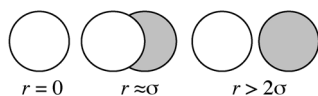


FIG. 2

The region excluded to sphere centres by two cavity sites separated by r . Each cavity site excludes sphere centres from a region of radius σ . The shaded region shows the change, $\Delta V(r)$, in the volume excluded when r is increased from 0 to r (Eq. (7))

The density of sphere centres within the shaded volume $\Delta V(r)$ shown in Fig. 2 can be approximated by the density $\rho g_{0c}(\sigma) = \rho g_{00}(\sigma)$ at the surface of a single cavity when $\Delta V(r)$ is small. The conditional probability, $n_{00}(r)/n_0 = n_0 g_{00}(r)$, that no centre lies in $\Delta V(r)$ is then $1 - \rho g_{00}(\sigma)\Delta V(r)$. The approximation becomes exact as $r \rightarrow 0$ so

$$n_0 g_{00}(r) = 1 - \rho g_{00}(\sigma)\Delta V(r) \quad \text{as } r \rightarrow 0. \quad (9)$$

Taking logarithms of both sides of Eq. (9), noting that $\ln(1-x) \rightarrow -x$ as $x \rightarrow 0$, gives

$$\ln[n_0 g_{00}(r)] = -\rho g_{00}(\sigma)\Delta V(r) \quad \text{as } r \rightarrow 0. \quad (10)$$

Differentiating Eq. (10) gives the slope at the origin

$$(d \ln[n_0 g_{00}(r)]/dr)_{r=0} = -\rho g_{00}(\sigma)(d\Delta V(r)/dr)_{r=0}. \quad (11)$$

Meeron and Siegert⁹ show that Eq. (10) is exact for hard rods in one dimension, for all $r \leq 2\sigma$, and that it yields the exact equation of state.

THERMODYNAMICS

With the geometrical terminology in place, we now explain some well known⁹⁻¹² relations between the geometrical and thermodynamic properties. The relations are explained with minimal use of statistical mechanics. They follow from classical thermodynamics and Boltzmann's equation $S = k_B \ln W$, where k_B is the Boltzmann constant and W counts the number of distinct microstates that contribute to the thermodynamic state¹.

The excess entropy, relative to an ideal gas with the same N , V and energy U , is

$$\Delta S = k_B \ln \Omega - k_B \ln \Omega_{\text{ig}}. \quad (12)$$

For the ideal gas, $\Omega_{\text{ig}} = \Omega_{\text{ig}}(N, V, \sigma = 0, \omega) = (V/\omega)^N/N!$. The kinetic energy, U , of the spheres is the same as that of the ideal gas, and an ideal gas particle has the same mass as a sphere, so the contribution to W from the many dis-

inct ways of distributing the kinetic energy among the particles¹ is the same in both cases and does not contribute to the difference ΔS .

For an isolated (N, V, U) system the chemical potential is $\mu = -T(\partial S/\partial N)_{V,U}$, where T is the temperature, and the excess chemical potential is

$$\Delta\mu = -T(\partial\Delta S/\partial N)_{V,U} = -k_B T(\partial\ln[\Omega/\Omega_{ig}]/\partial N)_{V,U}. \quad (13)$$

The derivative, $(\partial\ln\Omega/\partial N)_{V,U}$, is evaluated by noting that there are $V_{0,k}/\omega$ sites where another sphere can be added to configuration k of N spheres. The number of configurations of $N + 1$ spheres is the number of ways of adding a sphere to each configuration of N spheres, summed over all configurations, and divided by $N + 1$ because the added sphere is not distinguishable,

$$\Omega(N+1) = \sum_{k=1}^{\Omega(N)} \frac{V_{0,k}}{(N+1)\omega} = \frac{\Omega(N)V_0}{(N+1)\omega}. \quad (14)$$

Equation (14) gives the derivative

$$(\partial\ln\Omega/\partial N)_{V,U} = \ln\Omega(N+1) - \ln\Omega(N) = \ln\left[\frac{V_0}{(N+1)\omega}\right]. \quad (15)$$

For the ideal gas $V_0 = V$, so Eqs (13) and (15) yield

$$-\Delta\mu/k_B T = (\partial\ln[\Omega/\Omega_{ig}]/\partial N)_{V,U} = \ln[V_0/V]. \quad (16)$$

The factor $(N + 1)\omega$ in Eq. (15) cancels out in Eq. (16), so the result is the same whether the spheres are treated as distinguishable or indistinguishable, and the limit $\omega \rightarrow 0$ can be taken implicitly.

Equation (16), together with the definition $n_0 \equiv V_0/V$ and Eq. (8), gives

$$n_0 = \frac{1}{g_{00}(0)} = \exp\left[\frac{-\Delta\mu}{k_B T}\right] \quad (17)$$

which means that all the excess thermodynamic properties can be expressed in terms of the geometrical parameters n_0 or $g_{00}(0)$.

Boltzmann¹ calculated the chance that a pair of spheres are in contact by considering the probability that a sphere added to $V_{0,k}$ contacts the surface $S_{0,k}$ which is clearly proportional to $S_{0,k}/V_{0,k}$. A variation on Boltzmann's argument is used here to relate the pressure, P , to S_0/V_0 .

The set of all configurations of N spheres can be written as the sum of two sets

$$\Omega = \Omega_1 + \Omega_2 \quad (18)$$

where Ω_1 is the number of configurations in which no spheres are in contact and Ω_2 is the number of configurations with at least one pair of spheres in contact. A pair of spheres are said to be in contact when their centres are separated by σ to $\sigma + \delta\sigma$. $\delta\sigma$ cancels out of the result so the limit $\delta\sigma \rightarrow 0$ can be taken implicitly. The number of configurations in which no pair is in contact is the same as the number of configurations of a system of N spheres with diameter $\sigma + \delta\sigma$,

$$\Omega_1 = \Omega(N, V, \sigma + \delta\sigma, \omega) = \Omega + (\partial\Omega/\partial\sigma)_{N,V} \delta\sigma. \quad (19)$$

To evaluate the derivative in Eq. (19) we use the thermodynamic relation $P = T(\partial S/\partial V)_{N,U}$ and Eq. (12), which give

$$\frac{PV}{Nk_B T} - 1 = V \left(\frac{\partial(\Delta S/Nk_B)}{\partial V} \right)_{N,U} = \frac{V}{N} \left(\frac{\partial \ln[\Omega/\Omega_{ig}]}{\partial V} \right)_{N,U}. \quad (20)$$

$y \equiv \Delta S/Nk_B$ is an intensive quantity that depends only on the density variable $x \equiv N\sigma^D/V$, regardless of whether V or σ is the independent variable. With the straightforward manipulation $\partial y/\partial\sigma = (\partial y/\partial V)(\partial V/\partial x)(\partial x/\partial\sigma) = -(DV/\sigma)\partial y/\partial V$, and noting that $x = 0$ for the ideal gas, Eq. (20) gives

$$(\partial \ln \Omega/\partial\sigma)_{N,V} = -(ND/\sigma)(PV/Nk_B T - 1). \quad (21)$$

Equations (19) and (21) yield

$$\Omega_1 = \Omega[1 - (ND/\sigma)(PV/Nk_B T - 1)\delta\sigma]. \quad (22)$$

To calculate Ω_2 we first consider the number of ways, Ω_3 , of adding an N -th sphere to a system of $N - 1$ spheres with the constraint that it contacts another sphere. Ω_3 is the number of available sites within $\delta\sigma$ of the surface of the available space $S_{0,k}(N - 1)$, summed over all $\Omega(N - 1)$ configurations

$$\begin{aligned}\Omega_3 &= \sum_{k=1}^{\Omega(N-1)} S_{0,k}(N-1) \delta\sigma/\omega = \Omega(N-1) S_0(N-1) \delta\sigma/\omega \\ &= \Omega N \frac{S_0(N-1)}{V_0(N-1)} \delta\sigma\end{aligned}\quad (23)$$

where the last step uses Eq. (14).

To relate Ω_2 to Ω_3 , consider a particular configuration, k , of N spheres, which has sphere centres at sites labelled a and b . The spheres are not distinguishable, but sites are distinct. Removing a sphere from site a yields a different configuration of $N - 1$ spheres than removing a sphere from site b . Thus there are two distinct configurations of $N - 1$ spheres, one with site a empty, the other with site b empty, to which an N -th sphere can be added to the empty site to yield the same configuration, k , of N spheres. The sum in Eq. (23) therefore counts two distinct additions that yield the same configuration, k , of N spheres. The number of configurations containing at least one contacting pair is therefore

$$\Omega_2 = \Omega_3/2 = \Omega \frac{N S_0}{2 V_0} \delta\sigma\quad (24)$$

where the small difference between N and $N - 1$ is neglected.

Substituting Eqs (22) and (24) into Eq. (18) gives^{4,6}

$$\frac{PV}{Nk_B T} = 1 + \frac{\sigma S_0}{2D V_0}.\quad (25)$$

Equation (6), with $j = 0$, gives

$$\frac{\sigma S_0}{2D V_0} = \rho B_2 g_{00}(\sigma).\quad (26)$$

Equations (25) and (26) yield the familiar^{10,12} virial equation for the hard sphere pressure

$$\frac{PV}{Nk_{\text{B}}T} = 1 + \rho B_2 g_{00}(\sigma). \quad (27)$$

Thus, the relations between geometry and thermodynamics, Eqs (17), (25) and (27), follow from classical thermodynamics and statistical geometry without any use of statistical mechanics beyond Boltzmann's $S = k_{\text{B}} \ln W$.

EXPERIMENTAL

Fluids of $N = 13500$ spheres were simulated by the molecular dynamics method¹³, in a cubic cell with periodic boundaries. After compressing¹⁴ or decompressing an equilibrated fluid from a nearby density, it was equilibrated for $250N$ collisions and configurations were sampled during the next $1000N$ collisions. Neighbour lists were made of all pairs of spheres with centres separated by less than 2.1σ and the lists were remade before any sphere moved $\sigma/2$, so that only listed pairs can collide. The lists also facilitate the calculation of the $n_j g_{cj}(r)$ so, for convenience, we sampled configurations whenever the lists were remade.

Measurements were made at density $z = \rho\sigma^3/\sqrt{2}$ (the density relative to the close packed face-centred cubic crystal) from $z = 0.3$ to $z = 0.72$. The equilibrium freezing density¹⁵⁻¹⁷ is $z_f \approx 0.663$ and the fluid is near its metastable extremity at $z = 0.72$. It freezes too quickly¹⁵ to allow precise measurements when $z > 0.73$.

The probability $n_j g_{cj}(r)$, that a site at distance r from a sphere centre is a V_j site, was measured in the range $0 < r \leq \sigma$. The method used to calculate $n_j g_{cj}(r)$ is described in detail by Ballance and Speedy¹⁸. A randomly oriented line of length 2σ (the diameter of an exclusion sphere) was centred on each sphere centre and the number of sphere centres within σ of each of 200 equally spaced points on the line was counted. To improve the statistics the line was randomly reoriented 9 times for each sphere in each configuration sampled. In that way we sampled $N_s = 10^{8.1 \pm 0.5}$ points at each of 100 radial distances r from a sphere centre. The standard sampling error (SSE) in the calculation of $n_j g_{cj}(r)$

$$\text{SSE}(n_j g_{cj}(r)) = \left(\frac{n_j g_{cj}(r) - (n_j g_{cj}(r))^2}{N_s} \right)^{1/2} \quad (28)$$

is about 0.015% when $n_j g_{cj}(r) \approx 0.1$, increasing to 45% when $n_j g_{cj}(r) \approx 10^{-7}$. The results are more precise and extensive than previous calculations¹⁸⁻²⁰ of $n_0 g_{00}(r)$.

Simpson's rule was used for the integrals $jV_j = N \int_0^\sigma 4\pi r^2 n_j g_{cj}(r) dr$ to get the n_j , $j \geq 1$, and n_0 was obtained from Eq. (1). The S_j were calculated using Eqs (5) and (6).

RESULTS AND DISCUSSION

Figure 3 shows how $n_j(z)$ varies with the density z . $n_j(z)$ is known exactly in one dimension⁴, rough estimates have been made for hard discs⁴ and some previous simulation results are available for spheres^{18,21}.

The probability distribution for finding exactly j sphere centres within a spherical region of radius σ at density z , $n_j(z)$, would yield $n_0(z)$ and the thermodynamic properties through Eq. (17). The distribution $n_j(z)$ vs j is approximately²¹ Gaussian in j , but the Gaussian approximation is poor when n_j is small. Crooks and Chandler²¹ and Rowlinson and Woods²² discuss alternative distributions, one of which²¹ is shown to predict the chemical potential quite accurately when $z < 0.4$, but not at higher densities, where $n_0(z)$ is very small (Fig. 3). Discontinuities in $n_j(z)$ vs z across the freezing

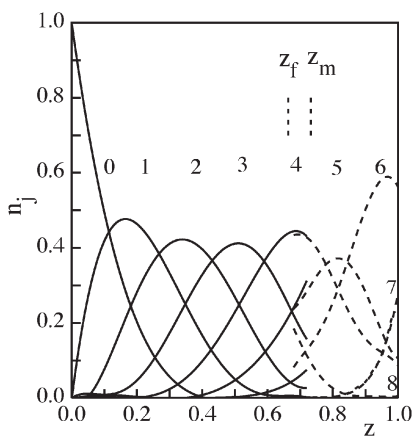


FIG. 3

The probability n_j that a site lies within j and only j sphere centres, versus the density z . Numbers show the value of j . Solid lines: fluid. Dashed lines: an fcc crystal of $N = 1372$ spheres with no vacancies. z_f and z_m show the equilibrium freezing and melting densities. Lines are polynomial fits

transition (Fig. 3) show that the form of the distribution is different in the fluid and crystalline phases.

Results for the cavity-cavity function $n_0 g_{00}(r)$ are shown in Fig. 4. Lines show the empirical form

$$\ln[n_0 g_{00}(r)] = -\Delta V(r)[a_1 + a_2 \Delta V(r)^\gamma]. \quad (29)$$

Equations (10), (11), (17), (27) and (29) are satisfied exactly with

$$a_1 = \rho g_{00}(\sigma) = (PV/Nk_B T - 1)/B_2 \quad (30)$$

and

$$a_2 = \{\Delta\mu/k_B T - \ln[g_{00}(\sigma)] - \rho g_{00}(\sigma)\Delta V(\sigma)\}/\Delta V(\sigma)^{\gamma+1}. \quad (31)$$

The value $\gamma = 3$ was found, empirically, to represent $n_0 g_{00}(r)$, $0 \leq r \leq \sigma$, precisely. The lines shown in Fig. 4 were drawn by calculating a_1 and a_2 from an accurate empirical equation¹⁵ for $PV/Nk_B T$ vs z , which also gives $\Delta\mu/k_B T$ by the thermodynamic integration

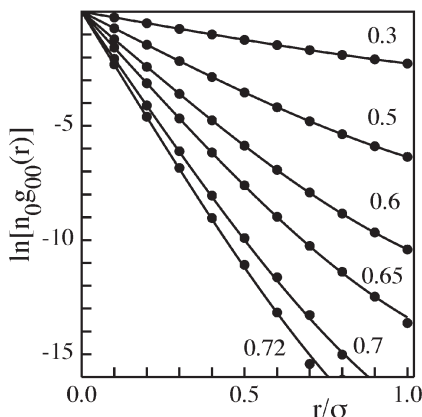


FIG. 4

$\ln [n_0 g_{00}(r)]$ versus r . $n_0 g_{00}(r)$ is the probability that a site at distance r from a cavity site is also a cavity site. Numbers show the density z . Lines represent Eq. (29)

$$\Delta\mu/k_B T = (PV/Nk_B T - 1) + \int_0^z (PV/Nk_B T - 1) d\ln z. \quad (32)$$

The smallest value shown in Fig. 4 is $\ln [n_0 g_{00}(r)] \approx -15$, where Eq. (28) gives a sampling error of about 0.2 in $\ln [n_0 g_{00}(r)]$, or twice the dot size in Fig. 4. For the other points, the sampling error is smaller than the dot size.

Figure 5 shows the deviation of the computed $n_0 g_{00}(r)$ from values calculated from Eq. (29). Most deviations are larger than the sampling errors estimated from Eq. (28). The systematic deviation evident at the lowest density studied, $z = 0.3$, is partly explained by the fact that configurations were sampled when the neighbour lists were remade, at which time a pair of spheres are in contact, rather than at a random time when the probability that a pair are in contact is small, particularly at low density. A rough estimate of the magnitude of that bias accounts for most of the systematic deviations shown at $z = 0.3$ in Fig. 5, and suggests that the bias is negligible when $z > 0.5$.

Equation (29) has obvious flaws. First, because it is analytic, it cannot show the discontinuities in the derivatives⁹ that occur whenever another sphere centre can fit within $\Delta V(r)$ as r increases. Second, extrapolating

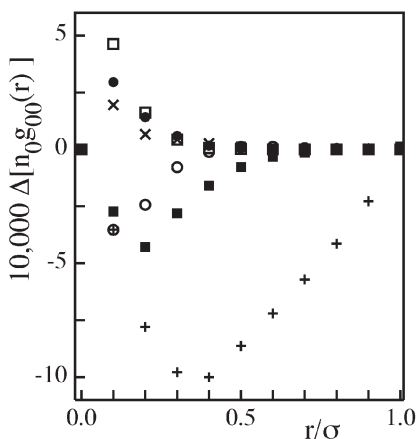


FIG. 5

Deviation of $n_0 g_{00}(r)$ from Eq. (29) (amplified by 10000) versus r , $z = 0.3$; ■, $z = 0.5$; ○, $z = 0.6$; ×, $z = 0.65$; ●, $z = 0.7$; □, $z = 0.72$

Eq. (29), with $\gamma = 3$, predicts that $n_0 g_{00}(r)$ decreases monotonically in the range $0 \leq r \leq 2\sigma$ and does not show the minimum²³ in $g_{cc}(r) = g_{00}(r)$ in the range $\sigma \leq r \leq 2\sigma$.

Heyes et al.²⁴ report precise calculations of the sphere-sphere radial distribution function, $g_{cc}(r)$, $r > \sigma$, and the slope $(d \ln g_{cc}(r)/dr)_{r=\sigma}$ at the contact distance, for densities $z \leq 0.716$. Figure 6 shows that their results are represented, within the scatter, by the values of $(d \ln g_{00}(r)/dr)_{r=\sigma}$ calculated from Eq. (29). This confirms that, although $n_0 g_{00}(r)$ is too small to be measured precisely when $r \approx \sigma$ and $z \geq 0.7$ (Fig. 4), Eq. (29) is accurate in that region.

Meeron and Siegert⁹ developed a hierarchy of integral equations relating the distribution function for n cavities to the distribution function for $n + 1$ cavities and they used an approximate closure to derive an equation of state. Smith and colleagues^{25,26} follow a similar approach to predict the equation of state and $n_0 g_{00}(r)$. Their prediction of $n_0 g_{00}(r)$ agrees²⁶ with earlier computed values²⁰ of $n_0 g_{00}(r)$ to within the computational uncertainties. A direct comparison of their predicted $n_0 g_{00}(r)$ (calculated from data in Table 1 of ref.²⁶) with our more precise computed values is not possible because the densities differ, however, the deviations of their predicted values²⁶ from Eq. (29) are larger than the deviations of our computed values from Eq. (29) at nearby densities.

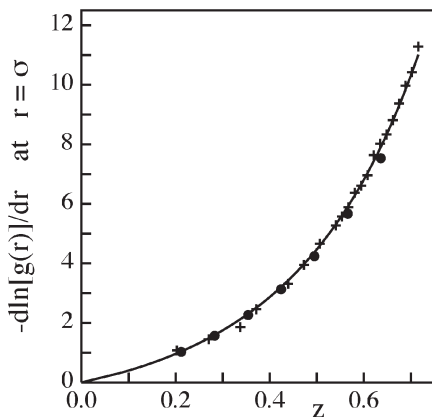


FIG. 6

$-d \ln [g(r)]/dr$ at $r = \sigma$, versus the density z . Crosses show data from Heyes et al.²⁴ Dots show values from Smith et al.²⁶ The line shows $-d \ln [n_0 g_{00}(r)]/dr$ at $r = \sigma$ from Eq. (29)

CONCLUSION

In summary, the cavity–cavity correlation function $g_{00}(r)$ is of interest because $g_{00}(0)$ and $g_{00}(\sigma)$ are related to each other through Eqs (17) and (27) and the thermodynamic relation between the chemical potential and the pressure⁹ (e.g., Eq. (32)). One more independent relation between them would yield the equation of state for hard spheres⁹. The simple empirical Eq. (29) represents our computed values of $g_{00}(r)$ precisely in the range $0 \leq r \leq \sigma$. It can be used to guide, and to test, attempts to find another relation between $g_{00}(0)$ and $g_{00}(\sigma)$.

We thank D. Heyes for supplying the data shown in Fig. 6. R. K. Bowles thanks NSERC and CFI for support.

REFERENCES

1. Boltzmann L.: *Lectures on Gas Theory*. University of California Press, Berkeley 1964.
2. Barker J. A., Henderson D.: *J. Chem. Phys.* **1967**, *47*, 4714.
3. Weeks J. D., Chandler D., Andersen H. C.: *J. Chem. Phys.* **1971**, *54*, 5237.
4. Speedy R. J.: *J. Chem. Soc., Faraday Trans. 2* **1980**, *76*, 693.
5. Speedy R. J.: *J. Chem. Soc., Faraday Trans. 2* **1977**, *73*, 714.
6. Speedy R. J.: *J. Phys. Chem.* **1988**, *92*, 2016.
7. Speedy R. J., Reiss H.: *Mol. Phys.* **1991**, *72*, 999.
8. Kirkwood J.: *J. Chem. Phys.* **1939**, *7*, 41.
9. Meeron E., Siegert A. J. F.: *J. Chem. Phys.* **1968**, *48*, 3139.
10. Hill T. L.: *Statistical Mechanics*. McGraw Hill, New York 1956.
11. Reiss H., Frisch H. L., Lebowitz J. L.: *J. Chem. Phys.* **1959**, *31*, 369.
12. Nijboer B. R. A., van Hove L.: *Phys. Rev.* **1952**, *85*, 777.
13. Alder B. J., Wainright J.: *J. Chem. Phys.* **1957**, *27*, 1208.
14. Lubachevsky B. D., Stillinger F. H.: *J. Stat. Phys.* **1990**, *60*, 561.
15. Speedy R. J.: *J. Phys.: Condens. Matter* **1997**, *9*, 8591.
16. Hoover W. G., Ree F. H.: *J. Chem. Phys.* **1968**, *49*, 3609.
17. Vega C., Noya E. G.: *J. Chem. Phys.* **2007**, *127*, 154113.
18. Ballance J. A., Speedy R. J.: *Mol. Phys.* **1985**, *54*, 1035.
19. Torrie G., Patey G. N.: *Mol. Phys.* **1977**, *34*, 1623.
20. Labík S., Malijevisky A.: *Mol. Phys.* **1984**, *53*, 381.
21. Crooks G. E., Chandler D.: *Phys. Rev. E* **1997**, *56*, 4217.
22. Rowlinson J. S., Woods G. B.: *Physica A (Amsterdam)* **1990**, *164*, 117.
23. Barker J. A., Henderson D.: *Mol. Phys.* **1971**, *21*, 187.
24. a) Heyes D. M., Cass M., Bránka A. C., Okamura H.: *J. Phys.: Condens. Matter* **2006**, *18*, 7553; b) Heyes D. M.: Private communication.
25. Labík S., Malijevisky A., Smith W. R.: *Mol. Phys.* **1994**, *83*, 983.
26. Smith W. R., Labík S., Malijevisky A., Sedlbauer J.: *Mol. Phys.* **1994**, *83*, 1223.